J. Plasma Physics (2013), vol. 79, part 6, pp. 1081–1087. © Cambridge University Press 2013
doi:10.1017/S0022377813001311

Low-dimensional relativistic degeneracy in quantum plasmas

M. AKBARI-MOGHANJOUGHI and A. ESFANDYARI-KALEJAHI

Department of Physics, Faculty of Sciences, Azarbaijan Shahid Madani University,
Tabriz 51745-406, Iran
(massoud2002@yahoo.com)

(Received 19 August 2013; revised 11 October 2013; accepted 14 October 2013; first published online 22 November 2013)

Abstract. In this work we investigate the effect of relativistic degeneracy on different properties of low-dimensional quantum plasmas. Using the dielectric response from the conventional quantum hydrodynamic model, including the quantum diffraction effect (Bohm potential) on free electrons, we explore the existence of the Shukla–Eliasson attractive screening and possibility of the ion structure formation in low-dimensional, completely degenerate electron–ion plasmas. A generalized degeneracy pressure expression for arbitrary relativity parameter in two-dimensional case is derived, indicating that change in the polytropic index (change in the equation of state) for the two-dimensional quantum fluid takes place at the electron number-density of $n_0 \simeq 1.1 \times 10^{20}\,\mathrm{cm}^{-2}$ whereas this is known to occur for the three-dimensional case in the electron density of $n_0 \simeq 5.9 \times 10^{29}\,\mathrm{cm}^{-3}$. Also, a generalized dielectric function valid for all dimensionalities and densities of a degenerate electron gas is calculated, and distinct properties of electron–ion plasmas, such as static screening, structure factor and Thomson scattering, are investigated in terms of plasma dimensionality.

1. Introduction

A large portion of recent literature belongs to the investigation of dense quantum plasmas with applications ranging from the low-density ultracold Rydberg plasma and the unitary Fermi gas to warm dense matter and astrophysical condensed hot matter (Shukla and Eliasson 2011; Shukla and Akbari-Moghanjoughi 2013). Recent improvements in quantum hydrodynamic (QHD) and quantum magnetohydrodynamic (QMHD) theories, including relativistic momentum, spin magnetization and wave–particle interaction features (Manfredi 2005; Shukla 2009; Shukla and Eliasson 2009; Shukla and Eliasson 2010), have turned the primary theories to one of the most useful theories for the investigation of diverse collective properties of dense fermionic systems, such as instabilities, localized excitations, light–matter interactions and optical and electrical properties of plasmas. Application of QHD theories has been shown to be capable of explaining some key features in quantum systems, such as quantum stream instability (Haas 2011), negative differential resistivity of semiconductors (Gardner 1994), white dwarf core-collapse beyond a critical mass-density (Akbari-Moghanjoughi 2013a), ordered structure formation in metallic density plasmas (Shukla and Eliasson 2012), warm dense matter (Glenzer et al. 2007) and many others.

One of the most important features of dense astrophysical plasmas is the relativistic degeneracy, which is the direct consequence of Pauli-exclusion and Heisenberg-uncertainty effects. In a compact star like a white dwarf, the internal electron pressure rises due to the existence of huge inward gravitational pull, which consequently leads to increase in electron momentum and kinetic energy. Since the electrons are fermions and degenerate quantum species confined to specific energy levels, their column collisions with other electrons are limited due to the Pauli-blocking mechanism, and the electron momentums become relativistic where their momentum becomes comparable with or even larger than their rest energy, a phenomenon known as the relativistic degeneracy (Chandrasekhar 1939). Therefore, as one moves deeper into a white dwarf, the gravitational pressure increases and the quantum degeneracy becomes more relativistic. The relativistic degeneracy is known to lead to many critical features of quantum plasmas such as the mass-limit and core-collapse in white dwarf stars (Chandrasekhar 1953, 1984), radical change in the equation of state of degenerate electron gas (Kothari and Singh 1942) and distinct features in linear and nonlinear wave dynamics (Akbari-Moghanjoughi 2010a, b). More recently, using the QHD approach, including the relativistic degeneracy and quantum diffraction effects on electron–ion plasmas, it has been shown that white dwarfs maximally scatter electromagnetic waves at the soft-Xray regime in their surface area with a typical mass-density of $10^6\mathrm{gr\ cm}^{-3}$ (Akbari-Moghanjoughi 2013b). On the other hand, real low-dimensional quantum plasmas or electron fluids are expected to be produced in the near future. In fact, such low-dimensional degenerate electron fluids are found in recently manufactured atom-thick monolayer graphene, carbon nanotubes or fullerene structures and

other allotropes of carbon with some extraordinary collective plasmon features (Castro Neto et al. 2009). We organize the paper as follows. A generalized dielectric function is calculated based on QHD model in Sec. 2. The static structure (SSF), radial distribution function (RDF) and Thomson elastic scattering cross section are calculated in Sec. 3. Discussion and summary are presented in Sec. 4.

2. The generalized hydrodynamic model and dielectric function

Consider an η-dimensional homogenous degenerate electron gas with a fixed inertial singly ionized ion background. We assume the plasma to be quasineutral and collisionless. Similar to the case of three-dimensional quantum plasma, the governing hydrodynamic equations are as follows:

$$\frac{dn}{dt}+n\nabla\cdot\mathbf{u}=0,$$
$$m_e\frac{d\mathbf{u}}{dt}=-e\mathbf{E}-\frac{1}{n}\nabla P_G+\frac{\hbar^2}{2m_e}\nabla\left(\frac{\Delta\sqrt{n}}{\sqrt{n}}\right), \quad (1)$$
$$\nabla\cdot\mathbf{E}=4\pi e(n_0-n),$$

where n, $\mathbf{u}$, $\mathbf{E}$ and P_G denote the number-density, the electron fluid velocity, the electrostatic field and the degeneracy pressure, respectively. The last force in the momentum equation corresponds to the Bohm potential, causing the collective electron wave interference and the Shukla–Eliasson attractive phenomenon. Other symbols, such as m_e, $\hbar$ etc., have their standard meanings. The generalized quantum degeneracy pressure, P_G, is a function of the relativity parameter, $R=p_{Fe}/m_ec$ (p_{Fe} being the relativistic Fermi-momentum) due to the fact that the electron relativistic velocity is a nonlinear function of the momentum, in general, i.e. $u=cx/\sqrt{1+x^2}$ with $x=p/m_ec$. This can be physically interpreted as if the electrons confined in a Pauli's quantum-box become relativistic as the external pressure or the electron number-density increases. To this end, we derive the generalized relativistic degeneracy pressure for the two-dimensional case by simply following the procedure for three-dimensional case (Chandrasekhar 1939). We use the general relation for the relativistic degeneracy pressure as

$$P_\eta=\frac{1}{\eta}\int_0^{p_{Fe}}pu(p)n_\eta(p)dp,\quad n_3(p)=\frac{8\pi p^2}{h^3},\quad n_2(p)=\frac{4\pi p}{h^2}, \quad (2)$$

where $\eta=1,2,3$ denotes the dimensionality of the system, and the number-densities, $n_\eta=\int_0^{p_{Fe}}n_\eta(p)dp$, for η-dimensions are $n_3=8\pi m_e^3c^3R_3^3/3h^3$, $n_2=2\pi m_e^2c^2R_2^3/h^2$ and $n_1=2m_ecR_1/h$, respectively. Therefore, we have $R_3=(n/n_{c3})^{1/3}$, $R_2=(n/n_{c2})^{1/2}$ and $R_1=(n/n_{c1})$ with $n_{c3}\simeq 5.9\times10^{29}\,\mathrm{cm}^{-3}$, $n_{c2}\simeq 1.1\times10^{20}\,\mathrm{cm}^{-2}$ and $n_{c1}\simeq 8.2\times10^{9}\,\mathrm{cm}^{-1}$ being relativity parameters for η-dimensional cases, respectively. In the forthcoming analysis we will avoid using the dimensionality index for n, for clarity. We readily derive the relativistic degeneracy pressures, P_η, as

$$P_3=\frac{\pi m_e^4c^5}{3h^3}\left[R_3\left(2R_3^2-3\right)\sqrt{1+R_3^2}+3\sinh^{-1}R_3\right],$$
$$P_2=\frac{2\pi m_e^3c^4}{3h^2}\left[2+\left(R_2^2-2\right)\sqrt{1+R_2^2}\right], \quad (3)$$
$$P_1=\frac{m_e^2c^3}{h}\left(R_1\sqrt{1+R_1^2}-\sinh^{-1}R_1\right).$$

Before proceeding, an important point needs clear attention. It might be argued that for the case of a relativistic degenerate plasma one should apply the fully relativistic hydrodynamics model, and the Bohm potential calculated from the non-relativistic approach is not appropriate in this context. However, this is not the case because the relativistic degeneracy of an electron gas starts at a mass-density of about $4.19\times10^6\,\mathrm{gr\ cm}^{-3}$ in the core of a 0.3 solar-mass white dwarf, which corresponds to the Fermi momentum, $P_{Fe}=1.29\ m_ec$ (or the relativistic degeneracy parameter value of $R_{03}=1.29$) or the threshold velocity of $u_{Fe}=0.63\ c$ with the Fermi relativistic factor of $\gamma_{Fe}=1.287$, indicating that one may safely use a QHD model, ignoring the relativistic electron dynamic features.

It is interesting to note in Fig. 1 that the polytropic index, γ_η, of the generalized pressure, $P_\eta/P_{0\eta}=(n/n_{c\eta})^{\gamma_\eta}$, has limiting values of $\{5/3,4/3\}$, $\{2,3/2\}$ and $\{3,2\}$ for the extreme non-relativistic and ultra-relativistic degenerate cases of $R_\eta=\{0,\infty\}$, respectively, for three- and two-dimensional electron fluids. On the other hand, we can also calculate generalized potential for the degeneracy pressure as $\Psi_\eta=\int(\partial_RP_\eta)/n_\eta dR_\eta=m_ec^2\sqrt{1+R_\eta^2}$. This is a surprisingly universal relation for all dimensionalities with R_η defined above in terms of the corresponding electron number-densities. Hence, we may apply the exact findings of Akbari-Moghanjoughi (2010b) to the two-dimensional case just with different definition for relativity parameter. Ignoring the Coulomb and electron exchange effects, we find the following static dielectric function for the two-dimensional degenerate electron fluid,

$$D_\eta(0,\mathbf{k})=1+\omega_{p\eta}^2\left[\frac{\hbar^2k^4}{4m_e^2}+T_\eta c^2k^2\right]^{-1},\ T_\eta=\frac{R_{0\eta}^2}{3\sqrt{1+R_{0\eta}^2}}, \quad (4)$$

where $\omega_{p\eta}=\sqrt{4\pi n_{0\eta}e^2/m_e}$ is the electron plasmon frequency and $R_{02}=(n_{02}/n_{c2})^{1/2}$ is the two-dimensional relativistic degeneracy parameter. Following the original work by Shukla and Eliasson (2012), we write the

https://doi.org/10.1017/S0022377813001311 Published online by Cambridge University Press

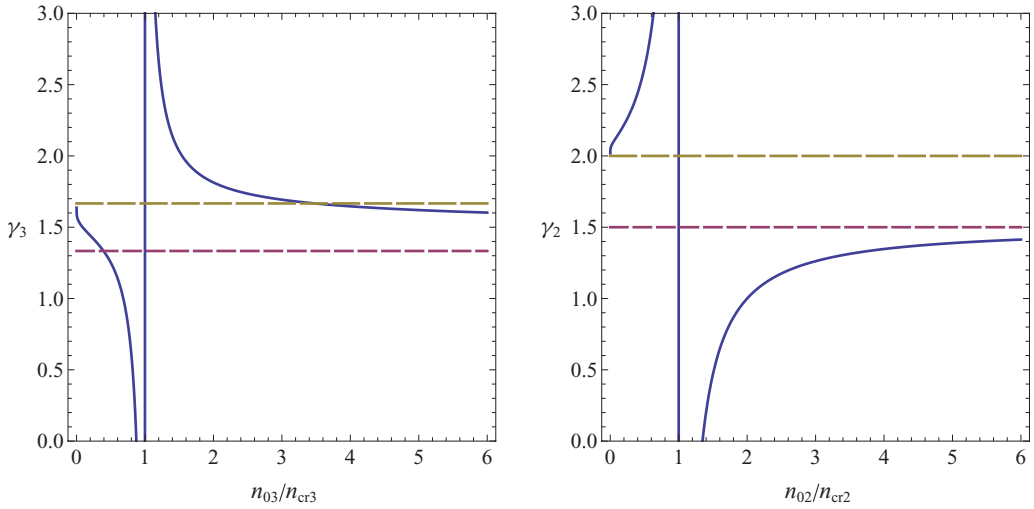

Figure 1. (Colour online) Variation of the polytropic index γ_η with respect to the normalized electron number-density for two- and three-dimensional quantum electron gas. The dashed lines correspond to the liming cases of $R_\eta = \{0, \infty\}$ for each dimension.

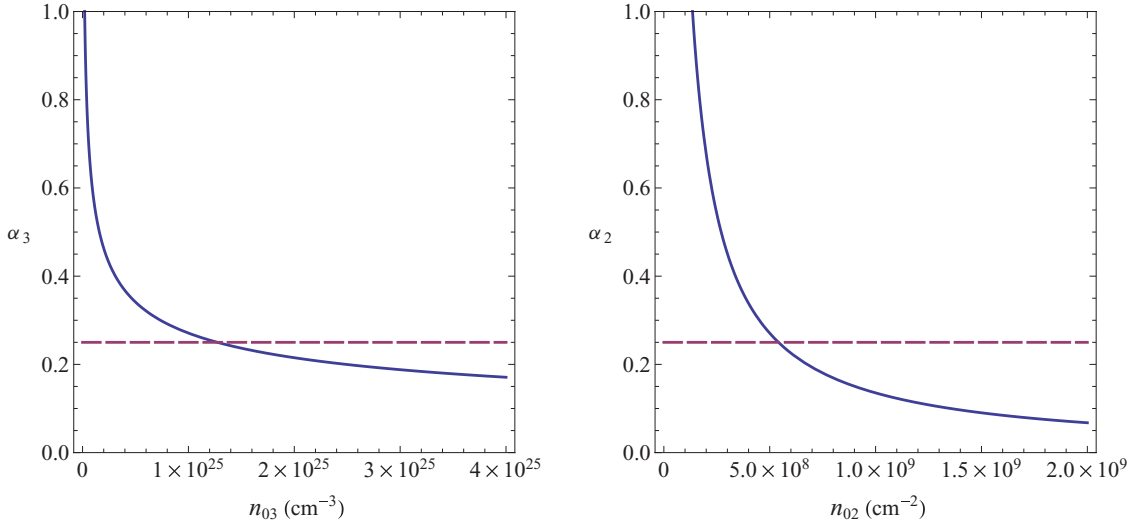

Figure 2. (Colour online) Variation of the Shukla–Eliasson potential parameter, α_η, with respect to the electron number-density, $n_{0\eta}$. The densities $\alpha_\eta > 1/4 (\alpha_\eta < 1/4)$ represent the attractive (repulsive) potential around the stationary positive test charge in quasineutral electron–ion quantum plasmas.

electrostatic potential as

$$\phi_\eta(r) = \frac{Q}{4\pi^2}\int\left[\frac{1+b_\eta}{k^2+k_{+\eta}^2}+\frac{1-b_\eta}{k^2+k_{-\eta}^2}\right]\exp(i\mathbf{k}\cdot\mathbf{r})d^\eta\mathbf{k}, \tag{5}$$

with the required parameters defined as

$$k_{\mp\eta}^2 = k_{0\eta}^2\frac{1\mp\sqrt{1-4\alpha_\eta}}{2\alpha_\eta}, \quad b_\eta = \sqrt{1-4\alpha_\eta},$$

$$\alpha_\eta = \frac{\hbar^2\omega_{p\eta}^2}{4m_e^2c^4T_\eta^2}, \quad k_{0\eta} = \frac{\omega_{p\eta}}{c\sqrt{T_\eta}}. \tag{6}$$

The positive stationary charge-screening potential for the case of a three-dimensional quantum electron gas is

$$\phi_3(r) = \frac{Q}{2r}\left[(1-b_3)\frac{e^{-k_{-3}r}}{r}+(1+b_3)\frac{e^{-k_{+3}r}}{r}\right], \tag{7}$$

where we have used the integration formula in spherical polar coordinate

$$\lim_{\nu\to0}\int_0^{2\pi}\left[\int_{-1}^{1}\left(\int_0^\infty\frac{\exp(ikr\mu-\nu k)}{k^2+k_s^2}k^2dk\right)d\mu\right]d\varphi = 2\pi^2\frac{e^{-k_sr}}{r}, \ \mu=\cos\theta. \tag{8}$$

On the other hand, for the screening potential of a two-dimensional electron gas, we obtain

$$\phi_2(r) = \frac{Q}{2\pi}\left[(1-b_2)K_0(k_{-2}r)+(1+b_2)K_0(k_{+2}r)\right], \tag{9}$$

https://doi.org/10.1017/S0022377813001311 Published online by Cambridge University Press

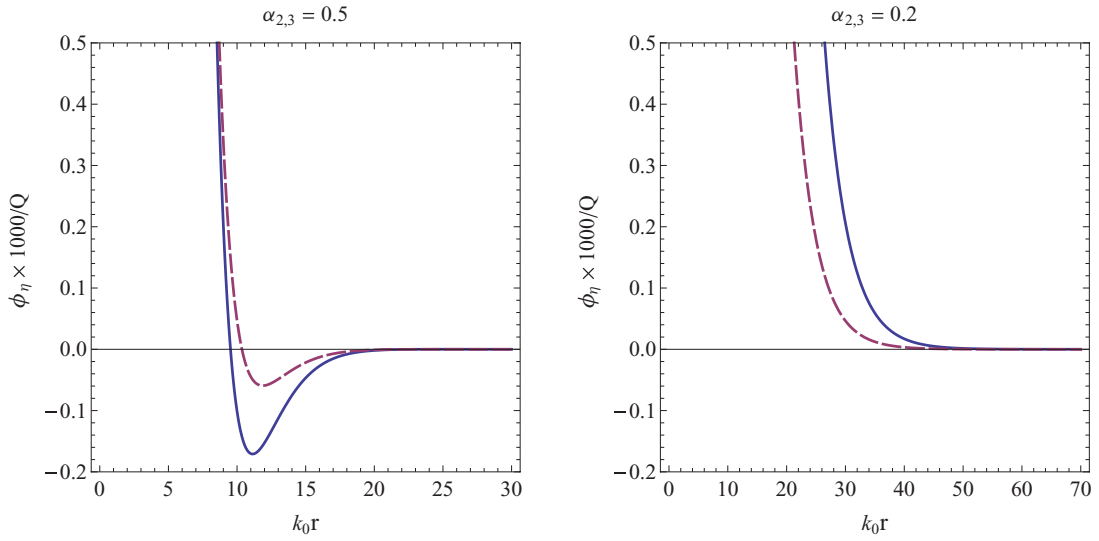

Figure 3. (Colour online) Electrostatic Shukla–Eliasson screening potential around a stationary positive charge Q within the two- (solid curves) and three-dimensional (dashed curves) quantum electron fluids. The attractive (the left plot) and repulsive (the right plot) indicate the transition of Fermi gases when the electron number-density value crosses the critical case of $\alpha_{0\eta} = 1/4$.

where we have used the integration formula in two-dimensional polar coordinate

$$\int_0^\infty \left(\int_0^{2\pi} \frac{\exp(\mathrm{i}kr\cos\theta)}{k^2 + k_s^2} \mathrm{d}\theta \right) k\mathrm{d}k = 2\pi K_0(k_s r), \quad (10)$$

with $K_0(r)$ being the Bessel K function of order zero. It is clearly observed that for all dimensionalities, the potentials ϕ_η turn over from attractive to repulsive when the parameter b_η turns from real to imaginary, or equivalently when the parameter α_η crosses the critical value of $\alpha_{\mathrm{cr}} = 1/4$. The $\alpha_\eta = 1/4$ value coincides with the electron number-densities of $n_{\mathrm{cr3}} = 1.3 \times 10^{25}\,\mathrm{cm}^{-3}$, $n_{\mathrm{cr2}} = 5.4 \times 10^{8}\,\mathrm{cm}^{-2}$ and $n_{\mathrm{cr1}} = 603\,\mathrm{cm}^{-1}$ for three, two and one dimensions, respectively. Figures 2 and 3 show the Shukla–Eliasson potential parameters α_η (and its variation with the electron number-density) and profiles in two- (solid profile) and three-dimensional (dashed profile) cases for different values of $\alpha_{2,3} = 0.5, 0.2$ corresponding to attractive and repulsive forces, respectively (note that the horizontal axis in these plots are not of the same scale but depend on $k_{0\eta}$, hence to the unperturbed electron number-density, $n_{0\eta}$). The value of $\alpha_{2,3} = 0.5$ corresponds to the densities of $n_{03} = 1.6 \times 10^{24}\,\mathrm{cm}^{-3}$ and $n_{02} = 2.7 \times 10^{8}\,\mathrm{cm}^{-2}$ for three and two dimensions, respectively. Also, the value of $\alpha_{2,3} = 0.2$ corresponds to densities of $n_{03} = 2.5 \times 10^{25}\,\mathrm{cm}^{-3}$ and $n_{02} = 6.8 \times 10^{8}\,\mathrm{cm}^{-2}$ for three and two dimensions, respectively.

Bearing in mind the above discussion, one has to critically inspect the applicability of the employed QHD model which uses the zero-temperature degeneracy assumption. For a fermion fluid to completely degenerate, we should have $\lambda_D > a_\eta$, where λ_D and a_η are the de Broglie thermal-wavelength $\lambda_D = h/\sqrt{2\pi m_e k_B T_p}$ (with the averageelectron temperature, $T_p = 300$ Kelvins in this paper) and the inter-particle spacing (the Wigner–Seitz cell radius) in the η-dimensional electron gas ($1/n_{03} = 4\pi a_3^3/3$, $1/n_{02} = 4\pi a_2^2$ and $1/n_{01} = a_1$) in η-dimensions, respectively. The de Broglie thermal-wavelength $\lambda_D = a_\eta$ leads to the densities of $n_{03} = 5.4 \times 10^{17}\,\mathrm{cm}^{-3}$, $n_{02} = 1.4 \times 10^{11}\,\mathrm{cm}^{-2}$ and $n_{01} = 1.3 \times 10^{6}\,\mathrm{cm}^{-1}$ for three, two and one dimensions, respectively. It is then clearly apparent that the zero-temperature assumption for degenerate electron gases is valid only for densities above $n_{02} = 1.4 \times 10^{11}\,\mathrm{cm}^{-2}$ and $n_{03} = 5.4 \times 10^{17}\,\mathrm{cm}^{-3}$. Therefore, for the three-dimensional electron gases, electron density of $5.4 \times 10^{17}\,\mathrm{cm}^{-3} < n_{03} < 2.5 \times 10^{25}\,\mathrm{cm}^{-3}$ satisfies the condition $\alpha_3 > 1/4$ and the zero-temperature assumption, and therefore for this density range one can have an attractive Shukla–Eliasson potential and ion structure formation. However, for the two and one-dimensional electron gases, the condition $\alpha_{1,2} > 1/4$ does not satisfy the complete degeneracy criteria. The variation of the Shukla–Eliasson parameter, α_{eta} with the electron number-density is depicted in Fig. 2 for two- and three-dimensional quantum electron gases. Hence, for one- and two-dimensional quantum electron gases, the charge screening potential is always of the Fermi–Thomas-like repulsive type (like the one shown in the right plot of Fig. 3) and there is no possibility of ionic structure formation in the absence of external confining potential. In the forthcoming analysis, we will avoid further discussion regarding the one-dimensional case, for clarity.

3. Ion correlations and the Thomson scattering

Let us now investigate the radial distribution function (RDF) of a two-dimensional electron gas that reflects ion structure in the plasma. Generalizing the findings

https://doi.org/10.1017/S0022377813001311 Published online by Cambridge University Press

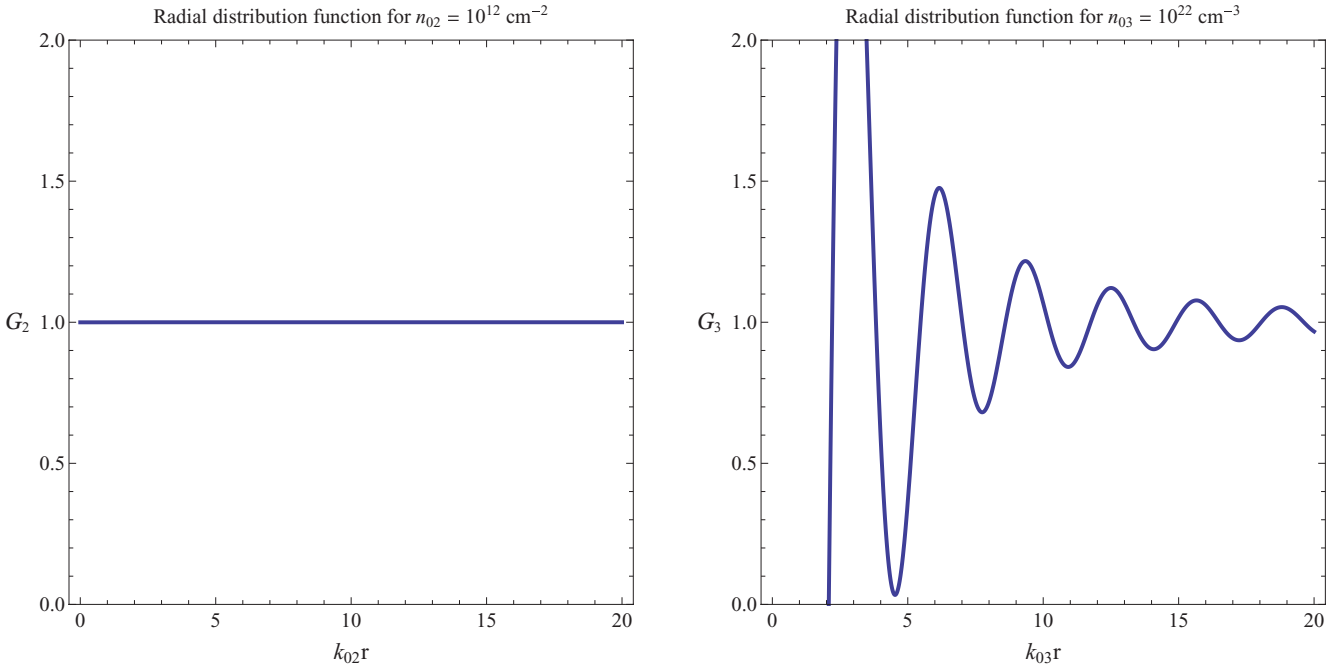

Figure 4. (Colour online) The radial distribution function (RDF) for two- and three-dimensional quantum electron fluids for typical number-densities relevant to each dimension. Strong oscillations for the three-dimensional case, which corresponds to the criteria of $\alpha_3 > 1/4$, indicates stronger ion correlations in this case.

of (Lee and Jung 2013), we see that the static structure factor of both two- and three-dimensional degenerate electron gas is given as

$$S_\eta(n_{0\eta}, \mathbf{K}_\eta) = \frac{K_\eta^2}{1 + K_\eta^2 + \alpha_\eta K_\eta^4}, \tag{11}$$

where the scattered wave-vector $\mathbf{K} = \mathbf{k}_f - \mathbf{k}_i$ [$K^2 = 2k^2(1 - \cos\Theta)$] with $\mathbf{k}_f$, $\mathbf{k}_i$ and Θ being the scattered wave-vector, initial wave-vector (in elastic scattering $k_i = k_f = k$) and the angle between them respectively, with K now being normalized to the value $k_{0\eta}$. The RDF is then given as

$$G_2(n_{02}, r) = 1 + \frac{k_{02}^2}{\pi n_{02}} \int_0^\infty K_2 \, [S_2(n_{02}, K_2) - 1] \frac{\sin K_2 r}{K_2 r} dK_2, \tag{12}$$

and

$$G_3(n_{03}, r) = 1 + \frac{k_{03}^3}{2\pi^2 n_{03}} \int_0^\infty K_3^2 \, [S_3(n_{03}, K_3) - 1] \frac{\sin K_3 r}{K_3 r} dK_3. \tag{13}$$

Using the standard definition for the differential cross section, we find that (Lee and Jung 2013)

$$\frac{d\sigma_{Th\eta}}{d\Omega} = N_\eta r_0^2 \left(1 - \frac{1}{2}\sin^2\Theta\right) S_\eta(n_{0\eta}, \mathbf{K}_\eta), \tag{14}$$

with N_η and Ω being the electron number and the conical scattering angle, and $r_0 = e^2/m_e c^2$ being the classical electron radius related to the standard electron scattering cross section, $\sigma_{0\eta}$, with $\sigma_0 = 8\pi r_0^2/3$. The reduced scattering cross section, $\bar{\sigma}_{Th\eta} = \sigma_{Th\eta}/N_\eta \sigma_{0\eta}$ then reads as

$$\bar{\sigma}_{Th\eta}(n_{0\eta}, k_\eta) = \int_{-1}^{1} \frac{K_\eta^2 [1 - (1 - \mu^2)/2] d\mu}{1 + K_\eta^2 + \alpha_\eta K_\eta^4}, \quad \mu = \cos\Theta. \tag{15}$$

4. Discussion and summary

Figure 4 depicts the radial distribution function for two- and three-dimensional degenerate electron gases and compares the profiles for two different values of electron number-densities relevant to each dimensionality. For the three-dimensional case, the number density of $n_{03} = 10^{22}\,\text{cm}^{-3}$ is a characteristic metallic solid density, and for the two-dimensional case, $n_{02} = 10^{12}\,\text{cm}^{-2}$ is a close value to the electron density of graphene (Hwang and Das Sarma 2007). It should be noted that recently Roldán et al. (in press) has used a similar hydrodynamic model to investigate the plasmon features of Dirac electrons in a monolayer graphene. It is observed that, while the RDF exhibits strong oscillations for a three-dimensional electron–ion plasma, the two-dimensional case lacks such a signature for charge correlations in the given plasma number-density.

In Figs. 5 and 6 we depict the variation of the normalized and differential Thomson scattering cross sections for different densities of two- and three-dimensional electron gases, respectively. It is clearly remarked that for both dimensionalities and all number-densities the Thomson scattering cross-section possesses well-defined maximum values (λ_m). These maximum optical responses

https://doi.org/10.1017/S0022377813001311 Published online by Cambridge University Press

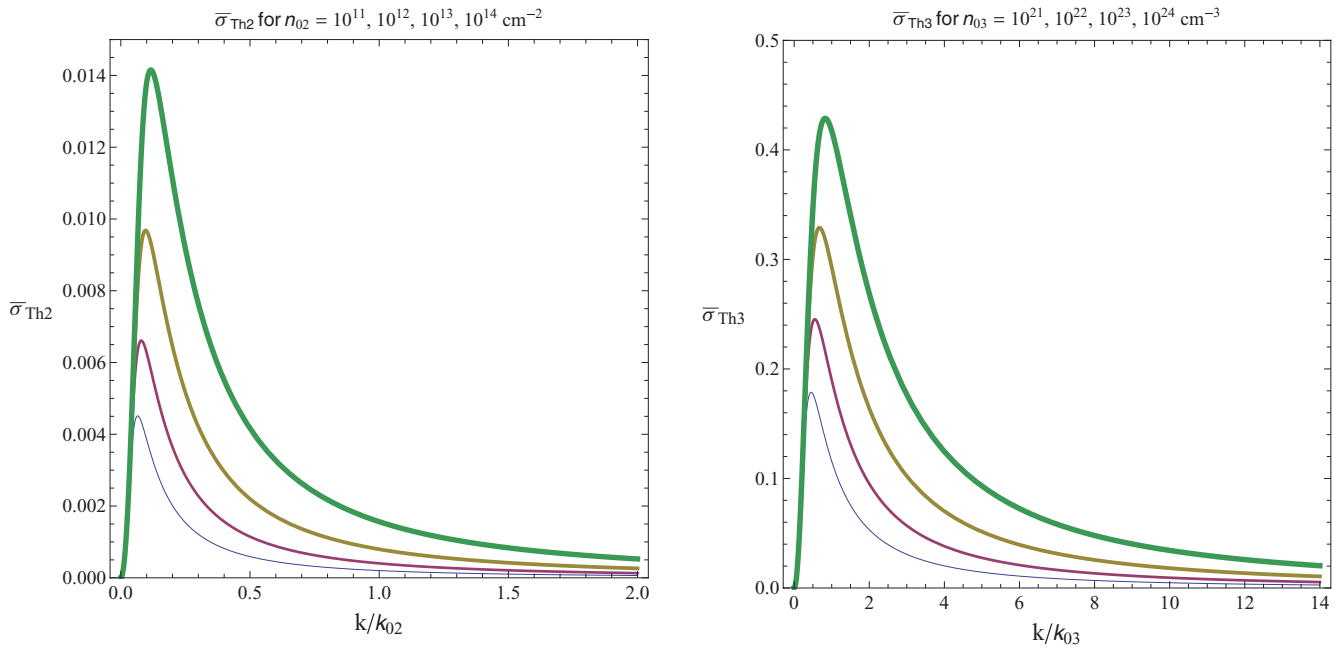

Figure 5. (Colour online) The normalized Thomson scattering cross section for two- and three-dimensional electron quantum fluids with different values of electron number-densities relevant to each dimensionality. It is observed that two- and three-dimensional degenerate electron gases respond well to the electromagnetic waves in microwave and X-ray frequency ranges, respectively.

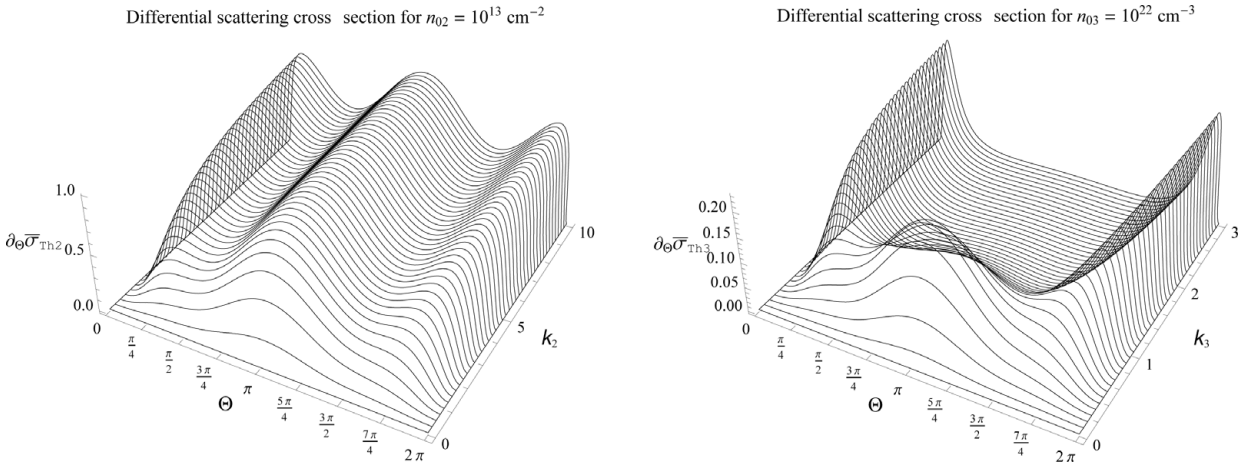

Figure 6. The differential Thomson scattering cross section for two- and three-dimensional electron quantum fluids with different values of electron number-densities relevant to each dimensionality. The angular variation of scattering profiles reveals fundamental differences between two dimensionalities.

reside typically at wavelengths of $\lambda_{m2} \simeq 190$ nanometers and $\lambda_{m3} \simeq 5$ Angstroms for $n_{02} = 10^{12}\,\mathrm{cm}^{-2}$ and $n_{03} = 10^{22}\,\mathrm{cm}^{-3}$ electron number-densities, respectively, increasing with increase in the electron number-densities for both two- and three-dimensional degenerate electron gases. These maximum scattering values are observed to tend to lower wavelengths. It is also observed that the scattering cross section for a two-dimensional quantum gas is typically much lower than that for the three-dimensional case. By a close inspection of Fig. 6, one notes a significant difference in differential cross section between the two- and three-dimensional quantum fluids with typical electron number-densities. It is observed that, while in the long wavelength limit for both dimensionalities there is a pronounced principal maxima at $\Theta = \pi$ in differential scattering profiles, with the decrease in the wavelength this maxima diminishes rapidly for the three-dimensional case, contrary to the two-dimensional case, in which the principal maxima persists up to a very high wavenumber values. It is also remarked that two other maxima around $\Theta = \pi/4$ and $\Theta = 7\pi/4$ are much sharper for a three-dimensional quantum electron fluid, compared with the two-dimensional case. The density dependence of the maximal Thomson scattering cross section is predicted to have important application in plasma diagnostics, laser-matter interactions and surface sciences.

https://doi.org/10.1017/S0022377813001311 Published online by Cambridge University Press

References

Akbari-Moghanjoughi, M. 2010a *Phys. Plasmas* **17**, 072101.

Akbari-Moghanjoughi, M. 2010b *Phys. Plasmas* **17**, 092304.

Akbari-Moghanjoughi, M. 2013a *Phys. Plasmas* **20**, 042706.

Akbari-Moghanjoughi, M. 2013b *Phys. Plasmas* **20**, 092902.

Castro Neto, A. H., Guinea, F., Peres, N. M. R., Novoselov, K. S. and Geim, A. K. 2009 *Rev. Mod. Phys.* **81**, 109.

Chandrasekhar, S. 1939 *An Introduction to the Study of Stellar Structure*, Chicago, IL: University of Chicago Press, 392 pp.

Chandrasekhar, S. 1953 *Mon. Not. R. Astron. Soc.* **113**, 667.

Chandrasekhar, S. 1984 *Science*, **226**, 4674.

Gardner, C. 1994 *SIAM, J. Appl. Math.* **54**, 409.

Glenzer, S. H., Landen, O. L., Neumayer, P., Lee, R. W., Widmann, K. and Pollaine, S. W. 2007 *Phys. Rev. Lett.* **98**, 065002.

Haas, F. 2011 *Quantum Plasmas: An Hydrodynamic Approach.* New York, NY: Springer.

Hwang, E. H. and Das Sarma, S. 2007 *Phys. Rev.* B, **75**, 205418.

Kothari, D. S. and Singh, B. N. 1942, Jul. 3 *Proc. R. Soc. London A Math. Phy. Sci.*, **180**(983), 414–423.

Lee, G. W. and Jung, Y.-D. 2013 *Phys. Plasmas* **20**, 062108.

Manfredi, G. 2005 *Fields Inst. Commun.* **46**, 263.

Roldán, R., Fuchs, J. N. and Goerbig, M. O. in press Collisionless hydrodynamics of doped graphene in a magnetic field. *Solid State Commun.* doi:10.1016/j.ssc.2013.04.011; arXiv:1305.1448 ; http://dx.doi.org/10.1016/j.ssc.2013.04.011.

Shukla, P. K. 2009 *Nature Phys.* **5**, 92.

Shukla, P. K. and Akbari-Moghanjoughi, M. 2013 *Phys. Rev.* E. **87**, 043106.

Shukla, P. K. and Eliasson, B. 2009 *Rev. Mod. Phys.* **83**, 25.

Shukla, P. K. and Eliasson, B. 2010 *Phys. Usp.* **53**, 51.

Shukla, P. K. and Eliasson, B. 2011 *Rev. Mod. Phys.* **83**, 885.

Shukla, P. K. and Eliasson, B. 2012 *Phys. Rev. Lett.* **108**, 219902 (E); Shukla, P. K. and Eliasson, B. 2012 *Phys. Rev. Lett.* **109**, 019901 (E).